Substitution effect on orientation of organosilicon compounds $(CH_3)_3SiX$ (X = F,Cl,Br,I,NCO) as studied using NEXAFS spectroscopy

2005 J. Phys.: Condens. Matter 17 5453

(http://iopscience.iop.org/0953-8984/17/36/002)

INSTITUTE OF PHYSICS PUBLISHING JOURNAL OF PHYSICS: CONDENSED MATTER

J. Phys.: Condens. Matter **17** (2005) 5453–5466 doi:10.1088/0953-8984/17/36/002

Substitution effect on orientation of organosilicon compounds $(CH_3)_3SiX$ (X = F, Cl, Br, I, NCO) as studied using NEXAFS spectroscopy

Tetsuhiro Sekiguchi[1], **Yuji Baba, Iwao Shimoyama, Krishna G Nath**[2] **and Md Nizam Uddin**[3]

Synchrotron Radiation Research Centre, Japan Atomic Energy Research Institute, Tokai, Naka, Ibaraki 319-1195, Japan

E-mail: sekiguch@popsvr.tokai.jaeri.go.jp

Received 15 June 2005, in final form 3 August 2005
Published 26 August 2005
Online at stacks.iop.org/JPhysCM/17/5453

Abstract

The orientation nature of multilayer organosilicon compounds has been investigated by measuring the dependence of the Si K-shell near-edge x-ray absorption fine structures (NEXAFS) on the polarization angle. Two approaches helped to elucidate the orientation mechanism: the substitution effect and the deposition-rate dependence. The orientation angles (α) of Si–X bond axes were obtained for trimethylsilyl halides, $(CH_3)_3Si$–X (X = F, Cl, Br, I, NCO), condensed on Cu(111) at a low (∼82 K) temperature: the angles are 60°, 73°, 61°, 55°, and 55° with respect to the surface normal, for X = F, Cl, Br, I, and NCO, respectively. Chloride (X = Cl) produces the most parallel tilt angle. The specific orientation nature of chloride is attributed to its strong dipole moment as well as the regular tetrahedron shape of the molecule. The molecular volumes calculated verify this view. Furthermore, deposition rates are found to greatly influence the growth manner: namely, high deposition rates led to a slightly perpendicular orientation of Si–X bond axis.

1. Introduction

The orientation of molecules on surfaces is not only an intriguing phenomenon in molecular science, but also an important issue in the development of high quality liquid crystals used as electronic display devices. Near-edge x-ray absorption fine-structure (NEXAFS) spectroscopy has been widely used to elucidate molecular orientation [13]. This method

[1] Author to whom any correspondence should be addressed.
[2] Present address: INRS-EMT, University of Quebec, Canada.
[3] Present address: Department of Chemistry and Applied Chemistry, Saga University, Japan.

becomes advantageous for non-crystalline systems, to which diffraction techniques cannot be applied. So far, much work has been done in terms of thin (mono- or bi-) layers on surfaces [2], while very few studies have attempted to clarify the orientation nature of thick multilayers. Many factors influence the orientation nature of thick layers: solid–solid and solid–surface interfacial free energies, deposition rate, and both the temperature and possible long-range influence of substrates [3]. This situation makes it difficult to establish a multilayer surface science. To address this subject, it is important to clarify factors that decisively influence multilayer structure.

For the present study, the authors focus on the effect of substitution of four ligands in silicon on multilayer orientation. Trimethylhalides and trimethylisocyanate, $Si(CH_3)_3X$ (X = –F, –Cl, –Br, –I, –N=C=O), were chosen as samples: the van der Waals radii are assumed to be I > Br > Cl > F. One expects that changing the van der Waals radius of each halogen will influence the ordering process and thus provide insight into the orientation mechanism. The silane derivatives have many applications. Organosilanes have been used for many years to improve the adhesion of polymers to oxidized substrates [8]. Physical and chemical properties presented here will provide information useful for the structural analysis of materials having halogen–silicon bonds.

Another intriguing feature of these silane compounds is that they are categorized as spherical-type molecules with a tetrahedral shape. A number of reports on dumbbell, e.g., O_2/graphite [4], disc [5, 6] and chain molecules, e.g., $(CH_3(CH_2)_{18}COO)_2X/Si(111)$ (X = Ca, Cd) [7], have shown that these shapes favour surface orientation. However, reports on spherical molecules have been quite scarce and it has not been established whether tetrahedral molecules show the orientation effect on surfaces or not.

We measured the average tilt angles of silicon–halogen (Si–X) bond axes for multilayers by NEXAFS spectroscopy and compared the angles from halide to halide. To further clarify the orientation property of these molecules, we carried out the NEXAFS measurements with varied deposition rates. The orientation characteristics will be discussed on the basis of the tilt-angle data, which depend significantly on the halogen substitution and on the deposition conditions.

2. Experiments

The NEXAFS measurements were carried out at the beamline-27A station at the Photon Factory in the High Energy Accelerator Research Organization. A double-crystal monochromator with InSb(111) was used, which gave an energy resolution of ≈0.9 eV at the Si K edge. The absolute photon energy was calibrated using a white line of solid SiO_2 [9]. A more detailed description of the apparatus used has been reported elsewhere [10]. Briefly, the apparatus was an ultrahigh vacuum (UHV) system (base pressure $\approx 1 \times 10^{-8}$ Pa) consisting of a quadrupole mass spectrometer (ULVAC MSQ-1000), a sputter ion-gun, and a cryogenic sample manipulator with liquid nitrogen. X-ray photoelectron spectra were measured using a hemispherical electron energy analyser (VSW CLASS-100). The NEXAFS spectra were recorded by measuring sample drain current as total electron yields (TEYs). The maximum sampling depth for the TEY method at the Si K edge has been reported to be ∼70 nm, indicating that the TEY probes averaged orientation of the condensed molecules lying from the surface to ∼70 nm deep regions [11]. All spectra were normalized to the values of the photon flux and the edge jump.

Commercially obtained high purity liquid-silane derivatives (Aldrich Co.) were used after the air was degassed. Cu(111) crystal was cleaned by repeated cycles of Ar^+ bombardment

and annealing at ∼800 K. Sample molecules were grown on the substrate cooled to 82 K using a gas-handling system [12]. This system allows control of the deposition rate and the total dose of sample gas and also diagnosis of the adsorbed samples using a thermal desorption spectroscope (TDS) (Eurothermo, type 818P4).

3. Results and discussion

3.1. The x-ray photoelectron spectra

We describe how we evaluated the thickness d of adsorbed molecules in the films that we prepared. Figure 1 shows wide spanned XPS spectra measured by 3200 eV photon excitation for varied layer thickness of condensed $Si(CH_3)_3Cl$. Assignments of peaks observed are indicated in figure 1, which include photoelectrons from substrate copper (Cu $2p_{3/2}$ and $2p_{1/2}$) and adsorbate molecules $Si(CH_3)_3Cl$ (Si 1s and Cl 1s), and Si KLL and Cl KLL Auger lines. As expected, the $I(\text{Si 1s})/I(\text{Cu } 2p_{3/2})$ ratio increases with the increase of sample gas dose. For homogeneous thin films covering the copper substrate, the intensity of Si 1s photoelectron $I(\text{Si 1s})$ is expressed as

$$I(\text{Si 1s}) = K\sigma(\text{Si 1s})\lambda_{\text{ads}}(\text{Si 1s})n(\text{Si})\left[1 - \exp\left\{\frac{-d}{\lambda_{\text{ads}}(\text{Si 1s})}\right\}\right] \tag{1}$$

where K is a constant depending the detection efficiency and the x-ray flux, $\sigma(\text{Si 1s})$ is the photoionization cross section of Si 1s at 3200 eV photons, $\lambda_{\text{ads}}(\text{Si 1s})$ is the inelastic mean free path (IMFP) of the Si 1s photoelectron in $Si(CH_3)_3Cl$ film and $n(\text{Si})$ is the atomic density of Si atoms [13]. For copper, the Cu $2p_{3/2}$ photoelectrons $I(\text{Cu } 2p_{3/2})$ are expressed as

$$I(\text{Cu } 2p_{3/2}) = K\sigma(\text{Cu } 2p_{3/2})\lambda_{\text{Cu}}(\text{Cu } 2p_{3/2})n(\text{Cu})\exp\left\{\frac{-d}{\lambda_{\text{ads}}(\text{Cu } 2p_{3/2})}\right\} \tag{2}$$

where all of the parameters are the same as those in equation (1). For σ, reported values were used [14]. The reported value of $\lambda_{\text{Cu}}(\text{Cu } 2p_{3/2})$, 29 Å, was used [15]. Using the TTP-2M equation [16], the values $\lambda_{\text{ads}}(\text{Si 1s})$ and $\lambda_{\text{ads}}(\text{Cu } 2p_{3/2})$ were estimated to be 46 and 71 Å, respectively. The $I(\text{Si 1s})/I(\text{Cu } 2p_{3/2})$ ratio calculated as a function of d is drawn in the upper part of figure 1. The calculated thickness is displayed above each spectrum. The error in the estimation of the film thickness was roughly 10%. Considering that the distance of one layer is approximately 5.9 Å,[4] the film thickness represented as spectrum (d) in figure 1 is estimated to be 60–70 molecular layers. The $I(\text{Cl 1s})/I(\text{Si 1s})$ ratio tends to be higher only in thin layers. This might suggest that some of the molecules are dissociatively adsorbed and chlorine molecules are desorbed. Dose amounts of all condensed samples discussed below were roughly three times magnitude greater than that for spectrum (d) in figure 1, which corresponds to ≈200 layers, thick enough to be able to ignore the thickness dependence.

3.2. The Si K-shell NEXAFS spectra

Figures 2(a)–(e) show the Si K-shell NEXAFS spectra of $Si(CH_3)_3X$ (X = F, Cl, Br, I, and NCO) in the grazing, intermediate, and normal incidence angles. A symbol 'θ' as shown in the inset of figure 2 represents the angle between the incident x-ray beam axis and the surface plane: the angle θ is also equal to the angle between the surface normal ($\vec{n}$) and the electric field vector (**E**) of the x-rays. The film of every compound was deposited by mostly the same

[4] The distance (l) of one layer was approximately estimated by the relation, $l = \sqrt[3]{P}$ where ρ is molar density in Å units (Å^3 mol^{-1}).

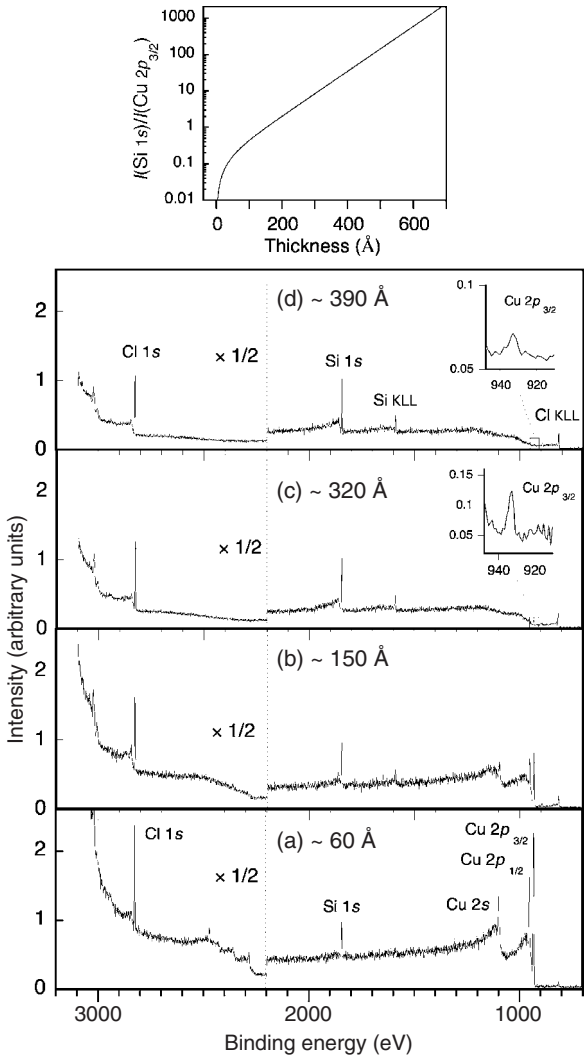

Figure 1. X-ray photoelectron spectra measured by the 3200 eV excitation for varied thicknesses of $Si(CH_3)_3Cl$ condensed on the copper substrate at 82 K. The all spectra are normalized to Si 1s peak intensity. The region for $E_b^F > 2200$ eV is multiplied by a factor of 0.5. Thicknesses estimated are indicated above the respective spectra. The inset is the expanded region around the Cu $2p_{3/2}$ peak.

dose rate and the thickness was approximately ∼200 molecular layers for all spectra. Three discrete resonances, denoted as **1**, **2**, and **3** in figures 2(a)–(e), were observed, and polarization dependence is obvious for the compounds with X = F, Cl, and Br, although we can barely discern the dependence for X = I. The variation of the intensity of these resonances with the incidence angle of polarized x-rays allows us to determine the orientation of the Si–X bond (C_3) axis. First we describe the characteristics of electronic transitions in the NEXAFS spectra on which the orientation analysis is based.

The Si K-shell NEXAFS of $Si(CH_3)_nCl_{4-n}$ ($n = 0$–4) has been systematically investigated in the gas phase [17] and in the condensed phase [18]. Because of the chlorine-substitution

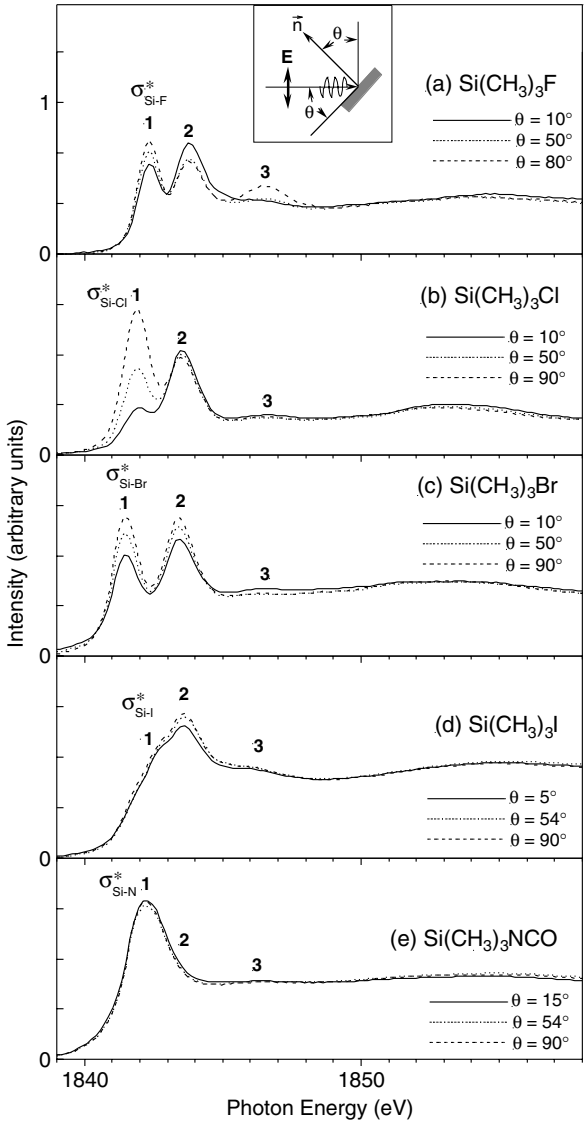

Figure 2. The Si K-shell NEXAFS spectra of $Si(CH_3)_3X$ ((a) X = F, (b) X = Cl, (c) X = Br, (d) X = I, and (e) X = NCO) condensed on Cu(111) at 82 K. The sample thickness was ∼ 200 layers for all spectra. Solid line (——), dotted line (· · · · · ·), and broken line (– – –) show the grazing ($\theta = 5°$ or 10°), intermediate ($\theta = 50°$ or 54°) and normal ($\theta = 80°$ or 90°) incidence angles, respectively. All spectra were normalized to the photon flux and the edge jump.

effect on the relative intensity ratio of the two resonances, peaks **1** at 1841.9 eV and **2** at 1843.5 eV in figure 2(b) were unambiguously assigned to Si 1s → σ^*_{Si-Cl} and Si 1s → $\sigma^*_{Si-CH_3}$ resonances, respectively. Since the Si 1s → σ^*_{Si-Cl} transition involves excitation of an electron from a spherical symmetric core state to the σ^*_{Si-Cl} molecular orbital localized along the Si–Cl (C_3) axis [17], the electronic transition probability of this resonance will be greatest when the electric field (**E**) vector is in the direction of this bond axis. In figure 2(b) the σ^*_{Si-Cl} resonance signals are enhanced in the normal incidence ($\theta = 90°$) in which the **E**

vector lies exactly parallel to the surface. This means that Si–Cl bond axes are preferentially parallel to the surface. Quantitative analysis to determine the tilt angles (α) is described in section 3.3.

For fluoride (X = F), peaks **1** and **2** seen in figure 2(a) were respectively assigned to Si 1s $\rightarrow \sigma^*_{\mathrm{Si-F}}$ and Si 1s $\rightarrow \sigma^*_{\mathrm{Si-CH_3}}$ resonances, based on the photon-stimulated desorption study of $Si(CH_3)_3F$ physisorbed on Cu(111) [19]. Excitation to resonance **1** gave rise to preferential dissociation of a Si–F bond, indicating that this excitation is relevant to a Si–F bond. The assignment is, furthermore, consistent with the NEXAFS [20], the photodissociation experiment [21], and the MS-Xα theory [20] of gas-phase $Si(CH_3)_nF_{4-n}$ (n = 0–4) in the Si L-edge region.

In analogy with the assignments described for chloride (X = Cl) and fluoride (X = F), we assume that peaks **1** and **2** for bromide (X = Br) and iodide (X = I) in figures 2(c) and (d) are attributable to Si 1s $\rightarrow \sigma^*_{\mathrm{Si-X}}$ and Si 1s $\rightarrow \sigma^*_{\mathrm{Si-CH_3}}$ resonances. It has been reported that two distinct resonances are observed in the C K-shell NEXAFS spectra of methyl halides CH_3X (X = Cl, Br, I) and that the C 1s $\rightarrow \sigma^*_{\mathrm{C-X}}$ and C 1s $\rightarrow \sigma^*_{\mathrm{C-H}}$ transitions account for the two resonances [22]. The transition characteristics of resonances **1** and **2** in trimethylsilyl halides in figures 2(a)–(d) are most probably analogous to those of methyl halides.

As shown in figure 2, or better visualized by deconvoluted components in figure 3, the positions of peak **1** depend on halogens and are shifted by ~0.9 eV from each other. As compared with peak **1**, those of peak **2** show relatively unchanged position within ~1843.6 ± <0.2 eV. The shape resonance relevant to the Si–X bond should more effectively be influenced by halogen substitution, than that relevant to the Si–C bond. Thus, this finding further supports our assignments of peaks **1** and **2**, respectively, to the $\sigma^*_{\mathrm{Si-X}}$ and $\sigma^*_{\mathrm{Si-CH_3}}$ shape resonances.

3.3. The orientation analysis of the NEXAFS spectra

To determine the average tilt angle of the Si–X bonds of $Si(CH_3)_3X$ condensed on Cu(111), the integrated intensities of the $\sigma^*_{\mathrm{Si-X}}$ resonance were obtained quantitatively by a curve-fitting technique. Using a nonlinear least-squares routine, the NEXAFS curves were fitted with a linear combination consisting of four symmetrically broadened Gaussian functions for the resonant features and of a Gaussian-broadened step function for the edge jump [23]. Typical spectral deconvolutions for $Si(CH_3)_3X$ (X = F, Cl, Br, I) are shown in figures 3(a)–(d).

For the Cu(111) substrate, the multilayer films are most unlikely to tend toward azimuth orientation with twofold symmetry. For systems with threefold or greater azimuth symmetry, the angle-dependent intensities for the $\sigma^*_{\mathrm{Si-X}}$ resonance can be expressed as [2]

$$I(\theta, \alpha) \propto P(\sin^2\alpha \sin^2\theta + 2\cos^2\alpha \cos^2\theta) + (1 - P)\sin^2\alpha \tag{3}$$

where P (=0.9) is the degree of linear polarization of x-rays and tilt angle α represents the angle between the Si–X bond axis and the surface normal direction ($\vec{n}$). (See the inset at the top in figure 4.)

Figures 4(a)–(e) show the experimentally derived relative intensities of the $\sigma^*_{\mathrm{Si-X}}$ resonance as a function of the x-ray incidence angles (θ). Also shown are lines calculated for three hypothetical α values. Using a non-linear least-squares method we obtained the averaged tilt angles (α) of Si–X bonds: 60° for X = F, 73° for X = Cl, 61° for X = Br, 55° for X = I, and 55° for X = NCO with respect to the surface normal ($\vec{n}$). The orientation for X = I and NCO is, however, indistinguishable from a random orientation because it is very close to the magic angle (α = 54.7°), at which no polarization dependence is expected.

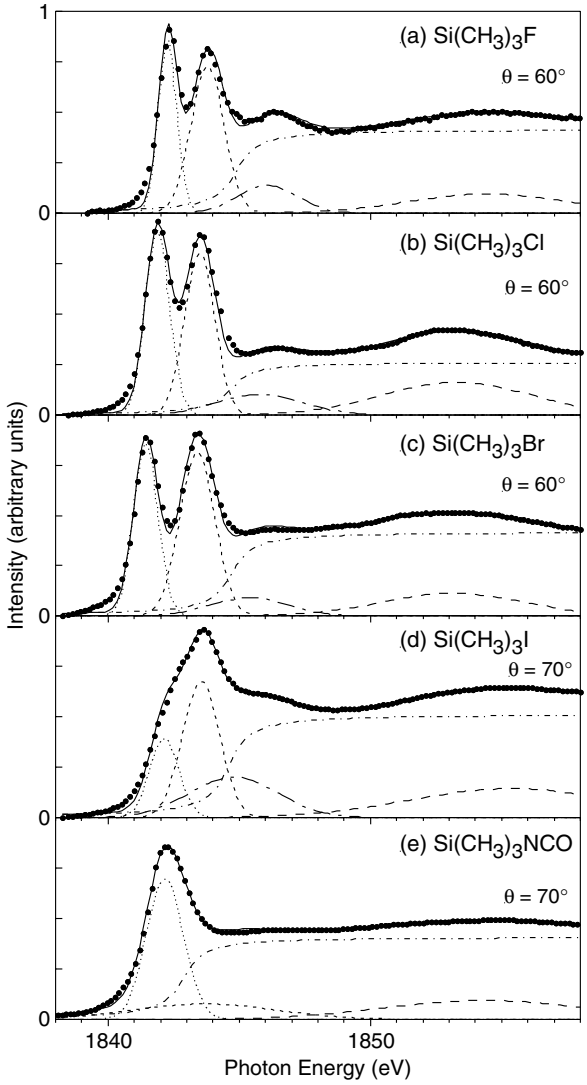

Figure 3. The spectral deconvolution for $Si(CH_3)_3X$ ((a) X = F, (b) X = Cl, (c) X = Br, (d) X = I, and (e) X = NCO) condensed on Cu(111) at ∼82 K. The incidence angles (θ) were written on the right of the spectra. The NEXAFS curves were fitted with linear combinations of four symmetrically broadened Gaussian functions for resonant features and a Gaussian-broadened step function for the edge jump.

It should be noted that most of all the substances show that the tilt angles between Si–X bond and the surface normal are at least larger than isotropic value, 54.7°, meaning that the orientation of the Si–X bond axes is preferred parallel to the surface. Although it is not surprising that two neighbouring molecules tend to align their dipoles in each microscopic region, the question remains as to why the preferential macroscopic orientation of Si–X axis becomes parallel to the surface. In the following we will give the present and previous facts as well as reference data for interpreting the orientation effect observed for our system.

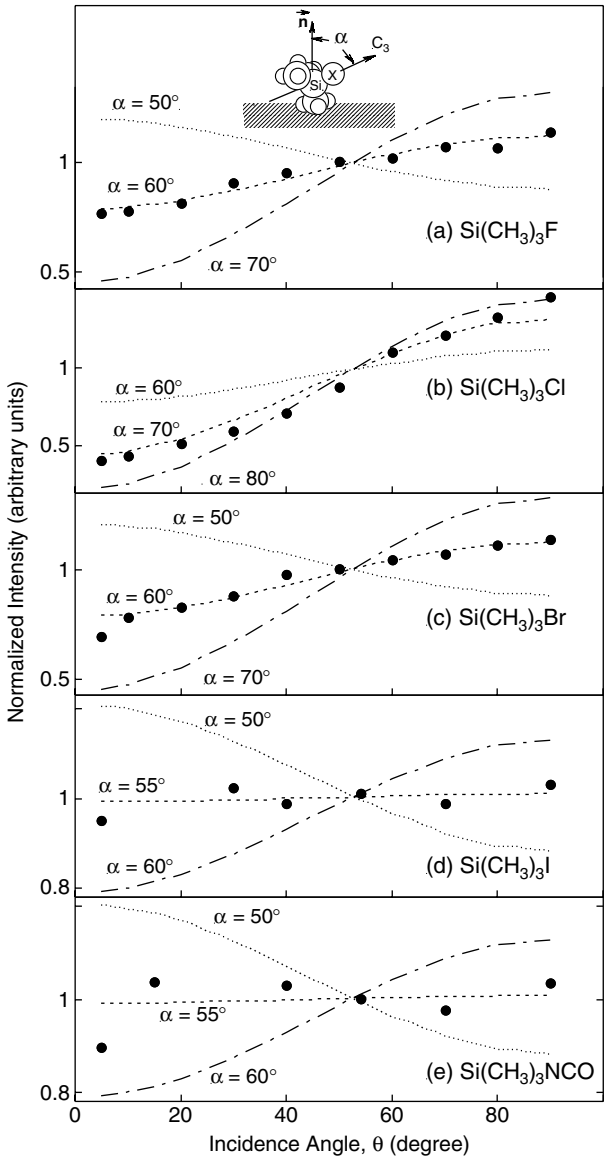

Figure 4. Intensity plot, $I(\theta)$, for the lowest ($\sigma^*_{\mathrm{Si-X}}$) resonance as a function of the x-ray incidence angles (θ). Also shown are calculated curves (dotted (· · · · · ·), broken (– – –), and chain (— · —) lines) for three hypothetical tilt angles (α) of Si–X bond axes. The tilt angles with respect to the surface normal are written beside the curves. $P = 0.9$ (P: polarization factor) was assumed.

First, $Si(CH_3)_3X$ (X = F, Cl, Br, I) studied here all have strong permanent dipole moment (μ) (approximately 1.6 D for every halide).[5] In addition, among condensed $Si(CH_3)_nCl_{4-n}$ (n = 0–4) molecules, only $Si(CH_3)_3Cl$, which has a high dipole moment, showed a strong

[5] Dipole moments (μ) of $Si(CH_3)_3X$ were estimated from those of SiH_3X, ($\mu = \sim$1.3 D) [23]. The μ of $Si(CH_3)_3X$ are estimated to be higher by ∼0.3 D than those of SiH_3X by the 'trimethyl' effect, considering that μ of $(CH_3)_3CX$ (X = Cl, Br, I) are higher by ∼0.3 D than the corresponding CH_3X (X = Cl, Br, I) [24].

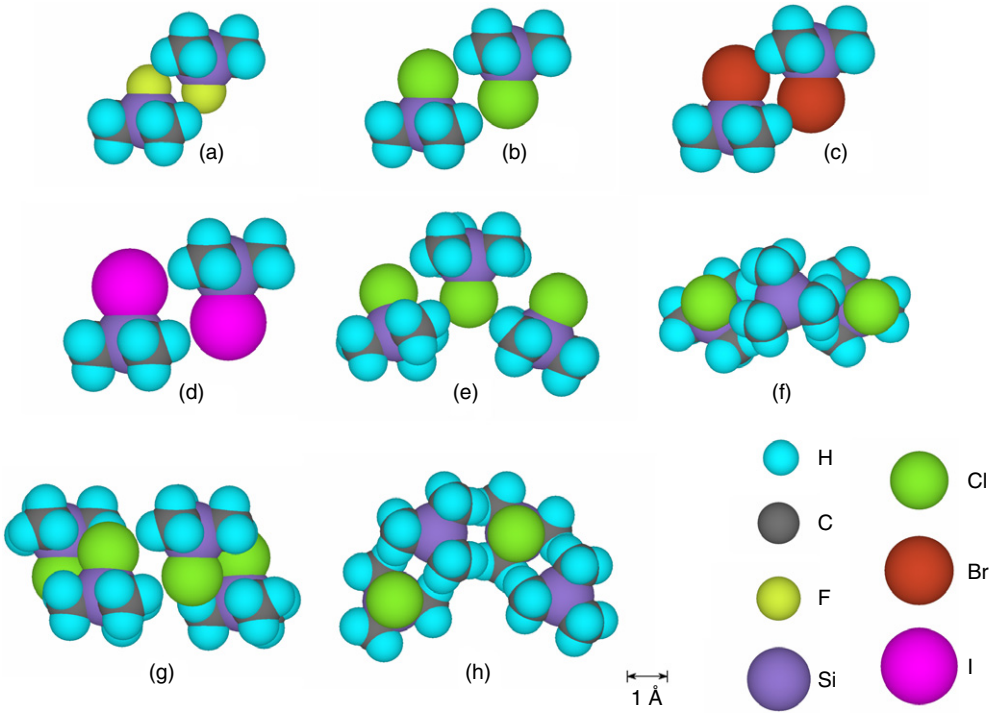

Figure 5. Globally optimized geometries of paired $(Si(CH_3)_3X)_2$ molecules ((a) X = F, (b) X = Cl, (c) X = Br, (d) X = I); parallel (e) and perpendicular (f) views of $(Si(CH_3)_3Cl)_3$ clusters; parallel (g) and perpendicular (h) views of $(Si(CH_3)_3Cl)_4$ clusters. For (a)–(d), the two Si and two X atoms are all in the same plane.

(This figure is in colour only in the electronic version)

angular-dependence in NEXAFS[6]. These facts strongly suggest that dipole interaction is an indispensable factor for the Si–X parallel orientation observed. We assume that Si–X bonds of two nearest-neighbouring molecules take anti-parallel geometry by dipole interaction and that overall parallel orientation originates as a result of the higher proportion of anti-parallel geometries at the near surface. Figure 5 shows globally optimized geometries of paired $Si(CH_3)_3X$ (X = F, Cl, Br, I) molecules interacting with each other, using *ab initio* Hartree–Fock molecular orbital calculation with a 6-31G basis set [25]. The molecular pairs, indeed, all favour anti-parallel orientation between Si–X bonds. It was also confirmed that this tendency is maintained for a cluster of four molecules (figures 5(g), (h)), although larger clusters are partially disordered. It should also be pointed out that molecular dynamics (MD) simulation has revealed that molecular dipoles align parallel to the surface at the liquid–vacuum interface of strong dipole molecules [27].

Second, the importance of the dipole interaction in the orientation effect, as mentioned above, is corroborated by the interfacial thermodynamics: the growth mode of thin films is generally determined by the solid–solid and solid–vacuum interfacial free energies. When the 'A'-terminated surface is covered by a monolayer with the 'B'-terminated surface, the free energy change $\Delta\gamma$ is described as follows:

$$\Delta\gamma_{A\to B} = \gamma_B + \gamma_{A-B} - \gamma_A \tag{4}$$

[6] This is readily expected on the analogy of CH_3Cl (1.87 D), CH_2Cl_2 (1.60 D), and $CHCl_3$ (1.01 D).

where γ_A and γ_B are surface free energies of the A-terminated surface and the B-terminated surface, respectively, and γ_{A-B} is an A/B interfacial energy arising mainly from strains at the A/B interface. The condition that such a film grows as a thermodynamically stable process is

$$\Delta\gamma_{A\to B} < 0. \tag{5}$$

Now we discuss the possibility of a growth process: a molecule sticking its halogen atom (X = Cl) upward covers molecules pointing their methyl (CH_3) groups to the vacuum. The free energy change that should be considered is

$$\Delta\gamma_{CH_3\to Cl} = \gamma_{Cl} + \gamma_{CH_3-Cl} - \gamma_{CH_3}. \tag{6}$$

Surface free energies for the silicon-halide derivatives treated here are not available; instead, those of (C)–Cl and (C)–CH_3 are available. Surface free energy for CH_3 termination (γ_{CH_3}) ranges from 20 to 22 mJ m^{-2} for solids [28]. The surface free energy of the –(CH_2–CHCl) structure (γ_{Cl}) is 39 mJ m^{-2} [28]. The strain term γ_{CH_3-Cl} is approximated with the following equation by Adamson [29]:

$$\gamma_{CH_3-Cl} = \gamma_{CH_3} + \gamma_{Cl} - 2\sqrt{\gamma^d_{CH_3}\gamma^d_{Cl}} \tag{7}$$

where $\gamma^d_{CH_3}$ and γ^d_{Cl} are interfacial energies contributed from dispersion forces[7]. We obtain $\gamma_{CH_3-Cl} \approx 2.7$ mJ m^{-2}. Equation (6) yields $\Delta\gamma_{CH_3\to Cl} \approx 20.7$ mJ m^{-2} (>0). This means that the growth case of equation (6) is thermodynamically unstable: a molecule sticking its halogen (Cl) upward is *unlikely* to lie on under-layers that have methyl (CH_3) groups pointing to the vacuum. In the same manner, we can readily prove that a counter-process is thermodynamically stable ($\Delta\gamma_{Cl\to CH_3} < 0$): a monolayer with the halogen (Cl)-terminated surfaces is *likely* to cover the methyl (CH_3)-terminated surfaces. The thermodynamic prediction made above is consistent with the observed orientation behaviour that halogen atoms tend not to point upright. Furthermore, the surface free energy for every halogen (F, Cl, Br, I) termination is always greater than that of methyl termination [28]. This explains the parallel orientation tendency in the film growth. We understand that the energy stabilization is caused due to strong dipole interaction induced by electronegativity of halogen atoms.

Although thermodynamic energetics predicts a rough tendency of parallel orientation, it does not explain a halogen-to-halogen comparison in the orientation angles observed as Cl > Br(≈F) > I. The surface free energies of halogen-containing molecules have the order F < Cl < Br < I [30]. Thus, this predicts that Si–I (iodide) would have the most parallel tilted bonds, but we have seen that this is not the case. Furthermore, contrary to the expectation that NCO induces the strongest dipole moment, it does not end in a substantial parallel orientation. These facts strongly suggest that dipole moment is not the only influential factor and another cause described below has to be taken into account.

We here introduce the concept of molecular shapes to interpret the orientation nature of our system. We assume that a regular tetrahedron shape of molecule tends to result in a regular lattice without distortion, which is postulated to strongly contribute to overall parallel orientation. To evaluate this point we calculated electron densities and molecular volumes of $Si(CH_3)_3X$ (X = F, Cl, Br, I) and compared them with that of tetramethylsilane ($Si(CH_3)_4$, i.e., X = CH_3), which has essentially a regular tetrahedron structure. The Gaussian 98 W *ab initio* molecular orbital program [25] was used. Optimized structures were obtained with the second-order Møller Plesset correlation correction (MP2) method with a 3-21G(d,p) basis set. The configuration interaction (CI) method with single excitation and with a 6-311G(d,p) basis set was used for electron densities and molecular volumes. The volumes of X = F, Cl, Br, I, and

[7] We tentatively use γ_{CH_3} and γ_{Cl} values as $\gamma^d_{CH_3}$ and γ^d_{Cl} considering that the dispersive force largely contributes to the surface free energy.

CH_3 were calculated to be 120.4, 146.5, 157.2, 177.6, and 138.1 $Å^3$ $molecule^{-1}$, respectively. It can be said that the volume of $Si(CH_3)_4$ is closest to that of chloride and is most different from that of iodide, thus the molecular shape of chloride most resembles that of $Si(CH_3)_4$. On the basis of the correlation between tilt angle and molecular shape, we conclude that the orientation tendency arises from not only dipole interaction, but also the regular tetrahedron shape of the molecule. We understand that the marked parallel orientation occurs as a result of a combination of two factors:

(1) strong dipole moment—it causes surface molecules to attract each other and the higher proportion of molecules tends to have anti-parallel geometry—and
(2) regular tetrahedron structure—it tends to have a more regular lattice without distortion than in a disordered tetrahedron system.

This explanation agrees nicely with the fact that some regular tetrahedral molecular solids are actually well crystallized: for example, solidified silicon tetrafluoride, SiF_4, and silicon tetraiodide, SiI_4 give a simple body-centred cubic structure [26]. Furthermore, the above-mentioned orientation tendency is in accordance with the fact that $Si(CH_3)_3NCO$, whose structure is much more different from a regular tetrahedron, does not show any marked parallel orientation. It is interesting to compare our system with disc-type molecules, 5-halouracil, $C_4H_3N_2O_2X$, (X = H, F, Cl, Br, I). It has been reported that uracil molecules (X = H) show a parallel orientation nature ($\alpha = 16°$ for X = H) with plane flat lying on the surface [31]. Plane angles are tilted up by halogen substitution: i.e., $\alpha = 23°$–$29°$ for X = Br and $\alpha = 32°$–$33°$ for X = I. This was ascribed to the effect that molecular ordering is hindered by the substitution of a hydrogen atom on the pyrimidine ring for halogen atoms with large van der Waals radii.

In the above discussion we did not take kinetic processes in growth into account. To clarify how the kinetic factor is involved in the orientation phenomenon, we performed the same experiments with various deposition rates. Figure 6 compares the NEXAFS spectra measured for two deposition rates ($\approx$3 Å s^{-1} for figure 6(a) and $\approx$10 Å s^{-1} for figure 6(b)) with a fixed thickness ($\approx$1600 Å) of $Si(CH_3)_3F$. It is clear that there is deposition-rate dependence as exhibited in the inset in figure 6. At lower deposition rates the parallel orientation is observed as mentioned so far, while at higher rates the orientation property is lost or even becomes slightly perpendicular to the surface. This observation suggests that not only a static factor (by dipole–dipole interaction) but also a kinetic factor affect the orientation nature. One of the possible explanations for this kinetic process is that a number of molecules are involved in the growth dynamics. If molecules land on the surface one by one, it is speculated that they have a certain length of time to completely settle into the most stable arrangement and have a chance of ending with preferential orientation. However, if multiple molecules come to the surface simultaneously, they would rarely be able to settle into the most stable site, the parallel orientation. Instead, they would end with random orientation. In addition, if the orientation occurs long after molecules land on the surface, the orientation angle should not depend on deposition rate: this is certainly not the case. Thus, we exclude the latter effect. Actually, the films were so stable that no time-dependent change of tilt angles was observed.

Here we have to comment on a role that the surface structure plays in the orientation effect. For mono- or thin layers, the origin of parallel or perpendicular orientation to the surface has been explained in terms of relative importance between molecule–substrate interaction and intermolecular interaction. The samples studied here, however, have thickness of $\approx$200 molecular layers, easily thick enough to be able to ignore the molecule–adsorbate interaction. For the chloride, $Si(CH_3)_3Cl$, the parallel orientation nature was so robust that it did not significantly depend on the cleaning procedure of the substrate. Moreover, we

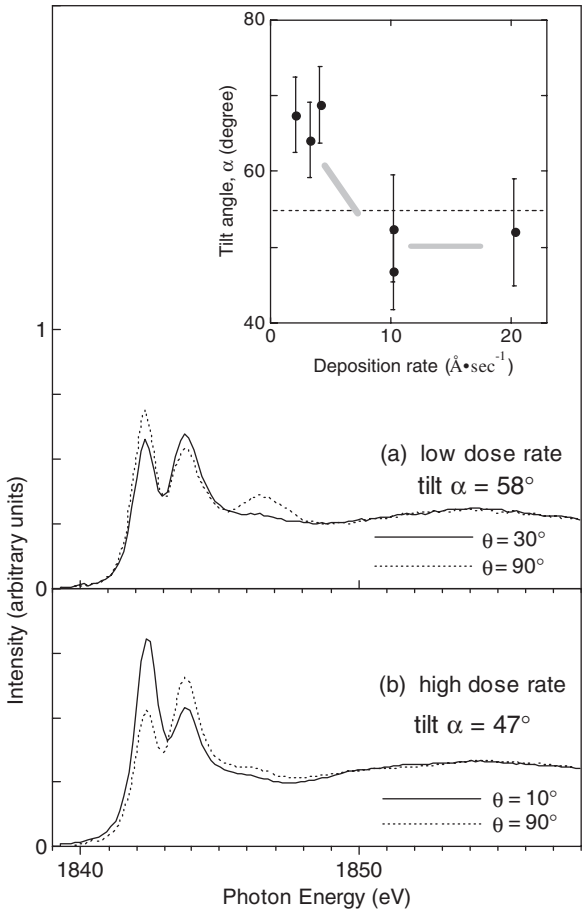

Figure 6. The NEXAFS spectra of $Si(CH_3)_3F$ with two different deposition rates with a fixed film thickness (≈1600 Å): (a) ≈3 Å s^{-1} and (b) ≈10 Å s^{-1}. The solid line (——) and dotted line (· · · · · ·) show the spectra for grazing incidence ($\theta = 10°$ or 30°) and normal incidence ($\theta = 90°$) angles, respectively. The inset at the top exhibits the measured Si–X tilt angles as functions of the deposition rates.

can compare our present results for $Si(CH_3)_3Cl$ on Cu(111) and on Cu(100) [32] with that of $Si(CH_3)_3Cl$ on Cu(110) in [18]. Despite the different facets of these substrates, their polarization-dependent NEXAFS data agree with each other quite nicely. According to the report, the $Si(CH_3)_3Cl$ sample condensed on Ni(111) and Pt(111) also gave the same parallel orientation as Cu(110) [18]. Furthermore, the same parallel orientation is observed for $Si(CH_3)_3Cl$ on thick (≈100 Å) cyclohexane (C_6H_{12}) buffered multilayers pre-dosed on cleaned Cu(100) [32]. All these pieces of evidence consistently exclude the possibility that the tilt angles are determined by the atomic-scale structure at the top surface of the substrates. We instead assume that intermolecular interaction in the near-surface region of molecular solids would rather be a possible driving force for the parallel orientation observed.

Further studies, for example MD simulations, are much needed to corroborate the above-mentioned conjectures, and measurements of systematic thickness dependence from mono-to multilayer film are in progress.

4. Summary

The orientation properties of condensed spherical-type molecules, $Si(CH_3)_3X$ (X = F, Cl, Br, I, NCO), were investigated by NEXAFS spectroscopy at the Si K-edge. The halogen-substitution effect on the one hand and the deposition-rate dependence on the other complemented the characterization of the molecular orientation nature. The observed findings and our views are summarized as follows.

(1) All silane compounds studied tend to form rather parallel oriented layers in a way that tilts the Si–X bonds toward the surface of the multilayers.
(2) The intermediate magnitude of a halogen (i.e. chloride) radius mostly favours the lying-down orientation of the Si–X bond: the anti-parallel geometry through strong dipole interaction with a regular tetrahedron shape of molecule most likely accounts for the parallel orientation nature.
(3) The deposition rate strongly influences the orientation nature: the parallel orientation behaviour shows up only when the slow layer-by-layer growth governs the kinetic process.

Acknowledgments

The authors would like to express their gratitude to the staff of the Photon Factory for their support. We are grateful to Dr H Yamamoto of JAERI and Ms N Hirao of NECO for their invaluable contributions to arranging and operating the BL-27A instruments. This work was undertaken with the approval of the Photon Factory Program Advisory Committee.

References

[1] Stöhr J and Jaeger R 1982 *Phys. Rev.* B **26** 4111
[2] Stöhr J 1992 *NEXAFS Spectroscopy* (*Springer Series in Surface Science* vol 25) (Berlin: Springer)
[3] Kondoh H, Matsui F, Ehara Y, Yokoyama T and Ohta T 2001 *Langmuir* **17** 817
[4] Guest R J, Nilsson A, Björneholm O, Hernnäs B, Sandell A, Palmer R E and Mårtensson N 1992 *Surf. Sci.* **269/270** 432
[5] Guay D, Tourillon G, Gastonguay L, Dodelet J P, Nebesny K W, Armstrong N R and Garrett R 1991 *J. Phys. Chem.* **95** 251
[6] Contini G, Carravetta V, Parent Ph, Laffon C and Polzonetti G 2000 *Surf. Sci.* **457** 100
[7] Kinzler M, Schertel A, Hähner G, Wöll Ch, Grunze M, Albrecht H, Holzhüter G and Gerber Th 1994 *J. Chem. Phys.* **100** 7722
[8] Plueddemann E 1982 *Silane Coupling Agents* (New York: Plenum)
[9] Baba Y, Sasaki T A and Yamamoto H 1994 *Phys. Rev.* B **49** 709
[10] Baba Y, Yoshii K and Sasaki T A 1995 *Surf. Sci.* **341** 190
[11] Kasrai M, Lennard W N, Brunner R W, Bancroft G M, Bardwell J A and Tan K H 1996 *Appl. Surf. Sci.* **99** 303
[12] Baba Y and Sekiguchi T 1999 *Surf. Sci.* **433–435** 843
[13] Carter W J, Schweitzer G K and Carlson T A 1974 *Electron Spectroscopy* ed R Caudano and J Verbist (Amsterdam: Elsevier Scientific) p 827
[14] Scofield J H 1973 *Lowrence Livermore Laboratory Report* UCRL-51326, TID-4500, UC-34, Physics 45
[15] Tanuma S, Ichimura S, Goto K and Kimura T 2002 *J. Surf. Anal.* **9** 285
[16] Tanuma S, Powell C J and Penn D R 1994 *Surf. Interface Anal.* **21** 165
[17] Ferrer J L, Bodeur S and Nenner I 1990 *J. Electron. Spectrosc. Relat. Phenom.* **52** 711
[18] Baba Y, Yoshii K, Yamamoto H and Sasaki T A 1995 *J. Phys.: Condens. Matter* **7** 1991
[19] Sekiguchi T and Baba Y 1999 *Surf. Sci.* **433–435** 849
[20] Bozek J D, Bancroft G M and Tan K H 1990 *Chem. Phys.* **145** 131
[21] Bozek J D, Tan K H and Bancroft G M 1991 *Chem. Phys.* **158** 171
[22] Lasky P J, Lu P H, Yang M X, Osgood R M Jr, Bent B E and Stevens P A 1995 *Surf. Sci.* **336** 140
[23] Outka D A and Stöhr J 1988 *J. Chem. Phys.* **88** 3539

[24] Lide D R (ed) 1998–1999 *CRC Handbook of Chemistry and Physics* 79th edn (Washington, DC: CRC Press) chapter 9, pp 42–9
[25] Frisch M J *et al* 1998 *Gaussian 98W, Revision A.7* (Pittsburgh, PA: Gaussian)
[26] Wyckoff R W G 1964 Crystal Structures *Inorganic Compounds* RX_n, R_nMX_2, R_nMX_3 vol 2 (New York: Wiley) p 127
[27] Dietter J and Morgner H 1996 *J. Phys.: Condens. Matter* **8** 3767
[28] Zisman W A 1963 *Ind. Eng. Chem.* **55** 18
[29] Adamson A W 1976 *Physics and Chemistry of Surfaces* 3rd edn (New York: Wiley)
[30] Jasper J J 1972 *J. Phys. Chem. Ref. Data* **1** 841
[31] Fujii K, Akamatsu K and Yokoya A 2004 *J. Phys. Chem.* B **108** 8031
[32] Sekiguchi T *et al* unpublished results